Molecular Crystals and Liquid Crystals

ISSN: 1542-1406 (Print) 1563-5287 (Online) Journal homepage: http://www.tandfonline.com/loi/gmcl20

The solidification behavior and phase equilibrium of o-Nitroaniline-β-Naphthol binary eutectic system

J. Singh & N. B. Singh

To cite this article: J. Singh & N. B. Singh (2016) The solidification behavior and phase equilibrium of o-Nitroaniline-β-Naphthol binary eutectic system, Molecular Crystals and Liquid Crystals, 624:1, 224-235, DOI: 10.1080/15421406.2015.1037553

To link to this article: http://dx.doi.org/10.1080/15421406.2015.1037553

Published online: 11 Feb 2016.

MOL. CRYST. LIQ. CRYST.
2016, VOL. 624, NO. 1, 224–235
http://dx.doi.org/10.1080/15421406.2015.1037553

Taylor & Francis
Taylor & Francis Group

The solidification behavior and phase equilibrium of *o*-Nitroaniline-β-Naphthol binary eutectic system

J. Singh and N. B. Singh

Research and Technology Development Centre, Sharda University, Greater Noida, India

ABSTRACT

Phase diagram studies of o-nitroaniline-β-naphthol system have been made by the thaw melt method. Simple eutectic type phase diagram was formed. Formation of eutectic mixture occurred at 0.7222 mole fractions of o-nitroaniline and melted at 326.85 K. The heat of fusion of components and eutectic mixtures were determined with the help of DSC technique and excess thermodynamic functions were calculated. Experiments were performed to study the undercooling, microstructure and linear velocities of crystallization. Flexural strength measurements were also made. Eutectic mixture showed higher flexural strength as compared to the components.

KEYWORDS

Enthalpy of fusion; entropy of fusion; eutectic; excess thermodynamic functions; flexural strength; microstructure; phase equilibria

1. Introduction

Various properties such as solidification behavior, mechanical strength, thermal properties, microstructures, etc. are very helpful in deciding the application of eutectic materials.[1–8] In addition, new reaction products are obtained when the reactions are carried out in eutectic melts.[9] Organic compounds having low melting temperature can be used as model systems. We have studied number of organic systems forming eutectics in order to understand their solidification behavior so that properties could be predicted.[3, 5, 7, 8, 10, 11]

In the present article, we have chosen o-Nitroaniline–β-Naphthol eutectic system for the study of their phase diagram, solidification behavior, and thermo chemical properties. The eutectic formed was characterized by DSC and FT-IR techniques. The microstructures of pure components and the eutectic have been predicted on the basis of Jackson's roughness parameter. Modulus of rupture of the eutectic and pure components was also determined to compare the flexural strength of eutectic mixture with those of the pure components.

2. Experimental procedure

2.1. *Materials and purification*

o-Nitroaniline (2-NAN) (KEMPHASOL, 98% pure) was purified by recrystallizing from hot water and the melting point was found to be 342.75 K (341.15–344.15 K literature value). β-Naphthol (2-NAPH) (MERCK, 98% pure) was used without any further purification and the

CONTACT N. B. Singh nbsingh43@gmail.com, n.b.singh@sharda.ac.in Research and Technology Development Centre, Sharda University, Greater Noida 201306, India.
Color versions of one or more of the figures in the article can be found online at www.tandfonline.com/gmcl.

Table 1. Temperature—composition data for o-NAN-β-NAPH system.

$X_{2\text{-NAN}}$	Solidus Temperature (T_S) (K)	Liquidus temperature (T_L) (K)	Temperature at which first nuclei appears (T) (K)	$\Delta T = T_L - T$ (K $\pm$ 0.0)
1.0000	–	342.75 $\pm$ 0.0	328.35 $\pm$ 0.0	14.4
0.9054	327.15 $\pm$ 0.0	341.65 $\pm$ 0.0	326.55 $\pm$ 0.0	15.1
0.8082	327.15 $\pm$ 0.0	338.45 $\pm$ 0.0	317.05 $\pm$ 0.0	21.4
0.7671	327.15 $\pm$ 0.0	334.95 $\pm$ 0.0	318.85 $\pm$ 0.0	16.1
0.7534	327.15 $\pm$ 0.0	331.65 $\pm$ 0.0	317.75 $\pm$ 0.0	13.9
0.7361	327.15 $\pm$ 0.0	330.45 $\pm$ 0.0	313.85 $\pm$ 0.0	16.6
0.7222*	—	326.85 $\pm$ 0.0	306.05 $\pm$ 0.0	20.8
0.7123	326.95 $\pm$ 0.0	331.75 $\pm$ 0.0	314.45 $\pm$ 0.0	17.3
0.6667	327.35 $\pm$ 0.0	340.25 $\pm$ 0.0	316.65 $\pm$ 0.0	23.6
0.6216	327.15 $\pm$ 0.0	345.05 $\pm$ 0.0	327.15 $\pm$ 0.0	17.9
0.5068	327.25 $\pm$ 0.0	357.55 $\pm$ 0.0	341.25 $\pm$ 0.0	16.3
0.4085	327.35 $\pm$ 0.0	364.35 $\pm$ 0.0	349.75 $\pm$ 0.0	14.6
0.3571	327.15 $\pm$ 0.0	368.85 $\pm$ 0.0	354.55 $\pm$ 0.0	14.3
0.3099	327.55 $\pm$ 0.0	371.95 $\pm$ 0.0	358.35 $\pm$ 0.0	13.6
0.2000	327.45 $\pm$ 0.0	379.45 $\pm$ 0.0	367.35 $\pm$ 0.0	12.1
0.1000	327.55 $\pm$ 0.0	385.35 $\pm$ 0.0	373.45 $\pm$ 0.0	11.9
0.0000	—	394.35 $\pm$ 0.0	385.55 $\pm$ 0.0	8.8

*Eutectic composition.

purity of the compound was checked by determining the melting point. The melting temperature was found to be 394.35 K (394.15–396.15 K literature value).

2.2. *Phase diagram studies*

The phase diagram of 2-NAN-2-NAPH system was studied by the thaw melt method.[12] The components were weighed in clean glass tubes in order to make mixtures of different compositions to an accuracy of $\pm$0.1 mg. Each glass tube was sealed in order to prevent the evaporation of the components and allowed to melt in a paraffin oil bath at a temperature slightly higher than the melting temperature of the components, shaken well and then chilled in ice cold water. Melting and chilling was repeated several times in order to have homogeneous mixtures. The solidified masses removed from the tubes were crushed into fine powders and their thaw and melting temperatures were recorded by using mercury thermometer. The composition, thaw and melting temperatures are given in Table 1.

2.3. *Undercooling measurements*

The undercooling measurements of various mixtures were made by the method described by Rastogi and Verma.[13] Accurate amounts of 2-NAN, 2-NAPH, and mixtures of different mole fraction were taken in clean glass tubes; the glass tubes were sealed and immersed in a paraffin oil bath maintained at a temperature slightly above their melting points. The heating was stopped on complete melting, and the bath was allowed to cool at a controlled rate. The formation of the first crystallite in the molten liquid was noticed by a magnifying glass. The difference between the true melting temperature and the temperature at which the first crystallite appeared gave the value of the undercooling temperature. The undercooling temperatures for different mixtures were recorded and are given in Table 1.

2.4. *Linear velocity of crystallization*

Linear velocity of crystallization for the pure components 2-NAN, 2-NAPH and eutectic were determined by the method described by Rastogi and Bassi.[12] The measurements were done

Table 2. Values of linear velocity of crystallization of o-NAN –β-NAPHbinary eutecticsystem at different undercooling (ΔT).

Components	k (mm s^{-1} K^{-1})	n
o-NAN	− 2.9753 (±0.0079)	0.1987 (±0.0029)
β-NAPH	− 3.0575 (±0.024)	0.611 (±0.0088)
Eutectic	− 3.2206 (±0.0026)	0.1083 (±0.0009)
Eutectic (mixture law)	− 3.1930 (±0.0454)	0.5045 (±0.0166)

in a cleaned U-shaped Pyrex glass tube of length 9 cm and diameter 0.5cm. The tube was filled with a solid material and kept in an oil thermostat at a temperature slightly above their melting temperatures. The linear velocities of solidification of components and eutectic mixture were determined at different undercooling by adding a seed crystal of the same compound through one side of the tube. After adding the seed crystal, nucleation followed by crystallization started. The length of the crystallized portion was measured as a function of time. Time required for crystallization for a definite length of the tube in the horizontal portion was recorded.

2.5. *Microstructural studies*

A small amount of fine powders of the two reactants, 2-NAN, 2-NAPH and Eutectic mixture were placed on separate glass slides, which were then kept in a dust-free container and heated in an oven at a temperature slightly above their melting temperatures, where the materials melted. The melts were crystallized by moving separate glass cover slips carefully over them in one direction. As a result, crystallization occurred and the microstructures were examined under a microscope. The photographs were recorded with the help of an optical microscope (OLYMPUS Chi 20) at a magnification of 10×. Microstructural studies were also made in the presence of impurities.

2.6. *Modulus of rupture measurement*

The modules of rupture of the samples were measured by the method described earlier.[14] The samples were melted in a uniform cylindrical glass tube at a temperature slightly higher than their melting temperatures, and then experimental tube were dropped vertically into ice bath maintained at ∼0°C. After complete solidification of the sample, the glass tube was slowly scrapped to give solid cylindrical shaped samples, made in a way similar to that as described earlier.[8] The modulus of rupture σ_{fs} of the materials were calculated with the help of Eq. (1)

$$\sigma_{fs} = \frac{F_f L}{\pi R^3} \tag{1}$$

where F_f is the load at fracture, L is the length of the cylindrical sample and R is the specimen radius. The strength values of pure components and the eutectic materials are given in Table 2.

2.7. *Differential scanning calorimetric*

Differential Scanning Calorimetric (DSC) studies of pure components, and eutectic mixture were performed using TG–DSC instrument, NETZSCH STA 409. Powders of samples were taken in alumina crucible with alumina lid and a blank crucible was taken as a reference.

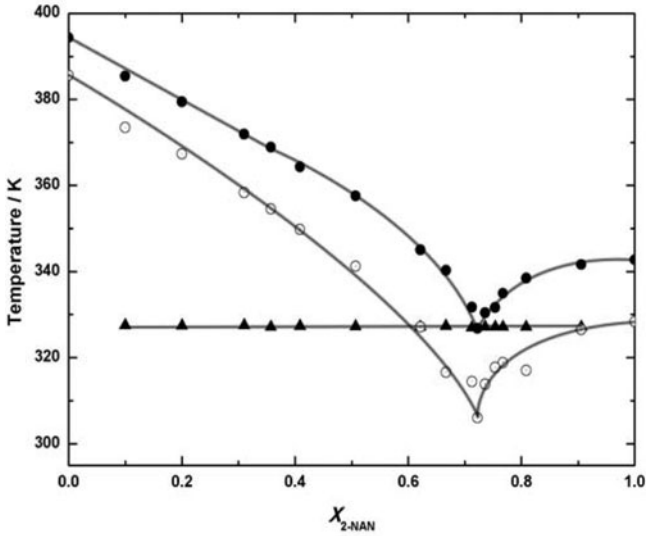

Figure 1. Temperature–composition diagram for 2NAN–2NAPH binary eutectic system: ▲, solidus temperature; •, liquidus temperature; ○, undercooling temperature.

The analysis was carried out in a nitrogen atmosphere from room temperature to 523 K at a heating rate of 5 K min^{-1}.

2.8. *FT-IR spectral studies*

FT-IR spectra of 2-NAN, 2-NAPH, Eutectic, were recorded with a FT-IR spectrophotometer in KBr phase.

3. Result and discussion

3.1. *Phase diagram*

The phase diagram of the 2-NAN—2-NAPH system is shown in Fig. 1. The temperature composition curve shows that a simple eutectic (melting point = 326.85K) at 0.7222 mol fraction of 2-NAN is formed. The eutectic point has two solid phases and a liquid phase in equilibrium. The undercooling curve was also constructed which is similar to the phase diagram curve shown in Fig. 1.

3.2. *Crystallization studies*

The linear velocities of crystallization (v) of the pure components and the eutectic mixture at different undercooling (ΔT), were found to obey the Hilling Turnbull Eq. 2.[15]

$$v = \mathrm{k}(\Delta T)^{\mathrm{n}} \tag{2}$$

where v is the linear velocity of crystallization, ΔT is the degree of undercooling, k is the kinetic coefficient and n is a crystallization parameter and depends on the solidification behavior of the materials.

When log v is plotted against log (ΔT), straight lines (Fig. 2) showing the validity of Eq. (2) are obtained. The values of k and n calculated from the lines are given in Table 2. The linear

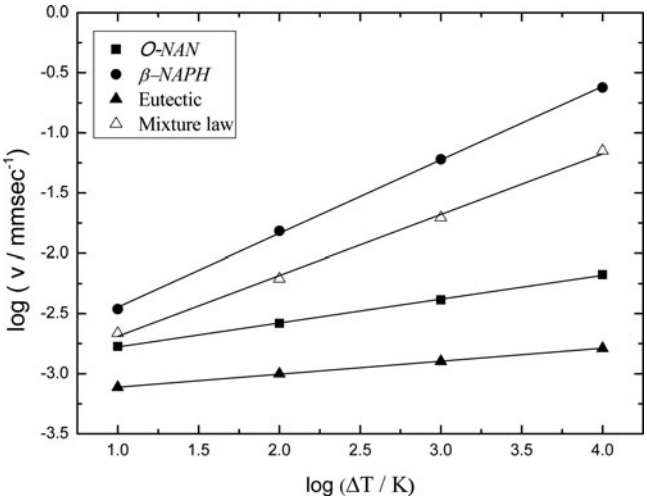

Figure 2. Verification of $v = k\,(\Delta T)^n$ in 2NAN—2NAPH system; ■, 2NAN; •, 2NAPH; ▲,Eutectic ; △, Eutectic ; (mix law).

velocity of crystallization (v) for the eutectic mixture was also calculated with help of mixture law (Eq. (3)) and is given in Table 2 and Fig. 2.

$$v_e = x_1 v_1 + x_2 v_2 \tag{3}$$

where x_1 and x_2 are the mole fraction of components 2-NAN and 2-NAPH and, v_e, v_1 and v_2 are the linear velocities of crystallization of eutectic mixture and pure components 2-NAN and 2-NAPH, respectively. It is found that at different undercoolings the linear velocities of crystallization calculated from the mixture law (Eq. (3)) for the eutectic mixture are higher than the experimental values (Fig. 2). It appears that in the eutectic mixture there may exist some weak interaction or molecular association between 2-NAN and 2-NAPH. As a result, the molecules of the components come closer and the eutectic mixture behaves like a bulky molecule. Because of this the rate of crystallization of the eutectic mixture is lower than that calculated by mixture law. The explanation for this could be given on the basis of Wingard theory [16] for the solidification of eutectics. According to this theory, the eutectic solidification begins with the formation of nucleus of one phase. This phase would grow until the surrounding liquid become richer in the other component and reaches at a stage when the second component starts nucleating. There are two possibilities of nucleation. The first possibility is side-by-side growth of the two components and the other possibility is alternate nucleation of the two initial crystals. In the first case, the rate of crystallization of eutectic materials is lower than that of the pure components, while in the second case, the linear velocity of crystallization of eutectic mixture is higher than that of any one of the two pure components. Therefore, in the present case there is a possibility of side-by-side growth of the two pure components.

3.3. *Thermal properties*

The enthalpy of fusion of the pure components and eutectic mixture are measured by DSC analysis (Fig. 3). The values of the enthalpies of fusion are represented in Table 3. If the solid eutectic mixture behaves ideally, its enthalpy of fusion can be calculated using mixture law, Eq. ():

$$(\Delta_f H)_{e,\text{mix law}} = (x_1)_e\,(\Delta_f H)_1 + (x_2)_e\,(\Delta_f H)_2 \tag{4}$$

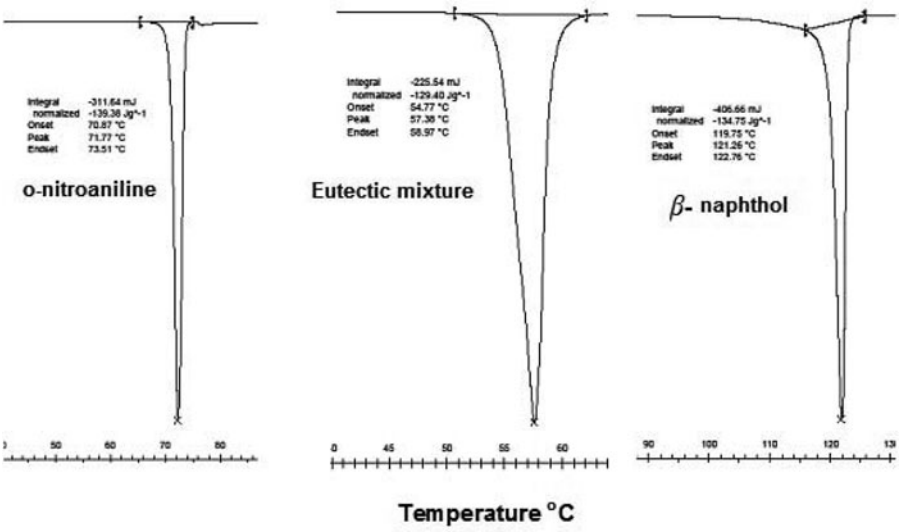

Figure 3. DSC curves of (a) 2-NAN, (b) Eutectic mixture and (c)2-NAPH.

Table 3. Values of enthalpy of fusion ($\Delta_f H$), interaction energy, and Jackson's Roughness parameter (α) for 2-NAN–2-NAPH binary eutectic system.

	$\Delta_f H$ (experimental)	$\Delta_f H$ (calculated by mixture law)	Interaction energy	Jackson's Roughness parameter (α)	
Component	(kJ mol^{-1})	(kJ mol^{-1})	(kJ mol^{-1})	$\xi = 0.5$	$\xi = 1.0$
o-NAN	19.25	–	–	3.3	6.8
β-NAPH	19.43	–	–	2.9	5.9
Eutectic	18.09	19.29	−1.2	3.3	6.7

where $(X_1)_e$ $(X_1)_e$ $(x_1)_e$ and $(X_2)_e$ $(x_2)_e$ are the mole fractions of the two components in the eutectic mixture and. $(\Delta_f H)_1$ and $(\Delta_f H)_2$ are the enthalpies of fusion of the pure components 1 and 2, respectively.

In the process of melting of eutectic mixtures, some sort of mixing and association may take place.[17,18] The enthalpy of fusion of eutectic mixture is related with enthalpy of mixing ($H_m{}^l$), solid–liquid interfacial energy ($\sigma_{LS}A$) and a constant ε, as given by Eq. (5).

$$\left(\Delta H_f\right)_e = \left[\left(\Delta H_f\right)_e\right]_{\text{mix.law}} + H_m^l + \sigma_{LS}A + \varepsilon \tag{5}$$

where $H_m^l + \sigma_{LS}A + \varepsilon$ is the total interaction energy which arises due to non-ideal nature of the eutectic mixture. The total interaction energy $\left(H_m^l + \sigma_{LS}A + \varepsilon\right)$ for each system is calculated employing Eq. (5).

Enthalpy of fusion for eutectic mixture is given in Table 3. The interaction energies for eutectic mixture is also calculated using Eq. (5) and are given in Table 3. There is difference in the values of enthalpy of fusion of eutectic mixture obtained from DSC studies and the mixture law value. This implies some sort of weak interaction between the components forming eutectic mixture.

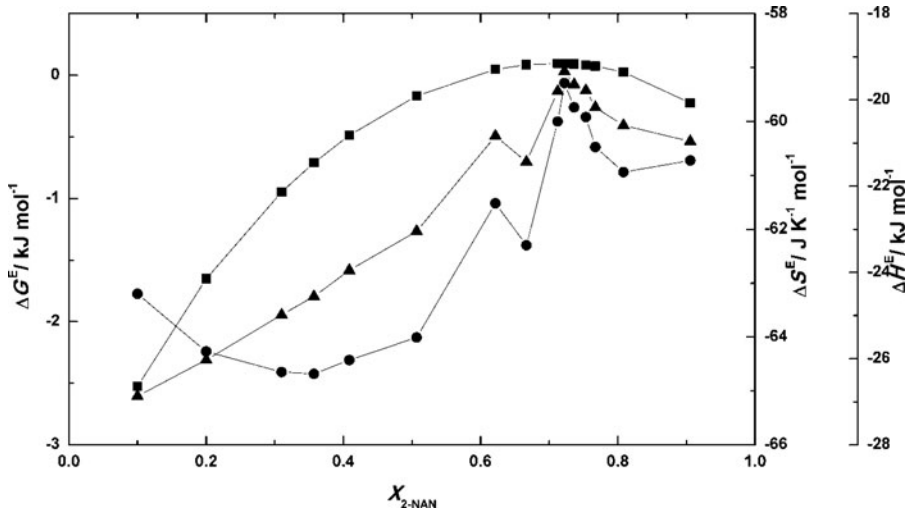

Figure 4. Values ΔG^E, ΔH^E and ΔS^E in 2NAN—2NAPH binary eutectic system:■, ΔG^E; •, $\triangle S^E$;▲,$\triangle H^E$.

3.4. *Thermodynamic properties*

Excess thermodynamic functions have been explored to understand the interaction between the components in a mixture. Excess Gibbs free energy (ΔG^E), excess entropy (ΔS^E), and excess enthalpy (ΔH^E) are calculated in a similar way as reported earlier[3,5,8,10,11] and plotted as a function of composition (Fig. 4)(Table 4). Values of ΔS^E and ΔH^E for entire range of composition are negative which indicate the non-ideal nature of the system. ΔG^E values for pre-eutectic composition is negative, whereas positive for eutectic and post-eutectic compositions. This reveals that the pre-eutectic compositions are more stable than eutectic and post-eutectic compositions.

3.5. *Microstructural studies*

The microstructural features in polyphase materials give shape, size and distribution of phases. These features control the electrical, mechanical, optical and other properties of a material. The microstructures (anisotropic) of 2-NAN, 2-NAPH and eutectic are given in Fig. 5. The microstructures of 2-NAN and eutectic mixture (Fig. 5) show that crystallization starts at a point and extends outside. On the other hand, the microstructure of 2-NAPH shows a rock type structure with cracks. Different impurities (1.0 wt%) changed the microstructure of eutectic mixture in a different way (Fig. 5). It appears that the presence of impurities of different nature affect the crystallization behavior in different ways.

Microstructures obtained by isotropic crystallization are different to some extent than the microstructures obtained by anisotropic crystallization (Fig. 6). It is possible that during isotropic crystallization, there is a freedom of crystallization in all the directions. As a result, the microstructures changed slightly.

The microstructures depend on various factors such as the nature and molecular structure of the components, interface contact angle between solid–liquid interface, concentration gradient, diffusion, nucleation characteristics and kinetic equilibrium characteristics of the two phases, chemical in homogeneities and type of defects present in stray crystals, voids and the growth twins. Since these parameters are very difficult to know precisely therefore it is not possible to predict the microstructure of the eutectic accurately. The growth morphology

Table 4. Excess Gibbs energy (ΔG^E), excess entropy (ΔS^E), and excess enthalpy (ΔH^E) for 2-NAN—2-NAPH binary eutectic system.

$X_{2\text{-NAN}}$	T_m K	$\ln\gamma_{2-\text{NAN}}$	$\ln\gamma_{2-\text{NAPH}}$	$\frac{\partial \ln\gamma_{2-\text{NAN}}}{\partial T}$	$\frac{\partial \ln\gamma_{2-\text{NAPH}}}{\partial T}$	ΔG^E (kJ mol^{-1})	ΔS^E (J K^{-1}mol^{-1})	ΔH^E (kJ mol^{-1})
0.9054	341.5	− 0.2082	1.1550	0.0035	0.1951	− 0.2249	− 60.7224	− 20.9616
0.8082	338.3	− 0.0946	0.4482	0.00132	0.1073	0.0267	− 60.9396	− 20.5891
0.7671	334.8	− 0.0424	0.2541	2.33816E−4	0.0922	0.0741	− 60.4752	− 20.1729
0.7534	331.5	− 0.0244	0.1969	− 1.54712E−4	0.0883	0.0832	− 59.9183	− 19.7797
0.7361	330.3	− 0.0012	0.1291	− 6.65996E−4	0.0839	0.0912	− 59.7371	− 19.6399
0.7222	327.7	0.0179	0.0778	0.0371	− 0.0185	0.0941	− 59.2876	− 19.3345
0.7123	331.6	0.0317	0.0428	0.0373	− 0.0171	0.0962	− 59.9981	− 19.7992
0.6667	340.1	0.0979	− 0.1044	0.0396	− 0.0078	0.0861	− 62.2950	− 21.4373
0.6216	344.9	0.1679	− 0.2313	0.0384	− 0.0118	0.0483	− 61.5176	− 20.8360
0.5068	357.4	0.3721	− 0.4963	0.0437	− 9.0884E−4	− 0.1669	− 64.0088	− 23.0437
0.4085	364.2	0.5877	− 0.6779	0.0490	0.0029	− 0.4874	− 64.4239	− 23.9506
0.3571	368.7	0.7222	− 0.7613	0.0529	0.0044	− 0.7098	− 64.6809	− 24.5577
0.3099	371.8	0.8639	− 0.8322	0.0577	0.0056	− 0.9476	− 64.6468	− 24.9832
0.2	379.3	1.3019	− 0.9799	0.0776	0.0078	− 1.6511	− 64.2671	− 26.0276
0.1	385.2	1.9950	− 1.0977	0.1336	0.0094	− 2.5251	− 63.1964	− 26.8683

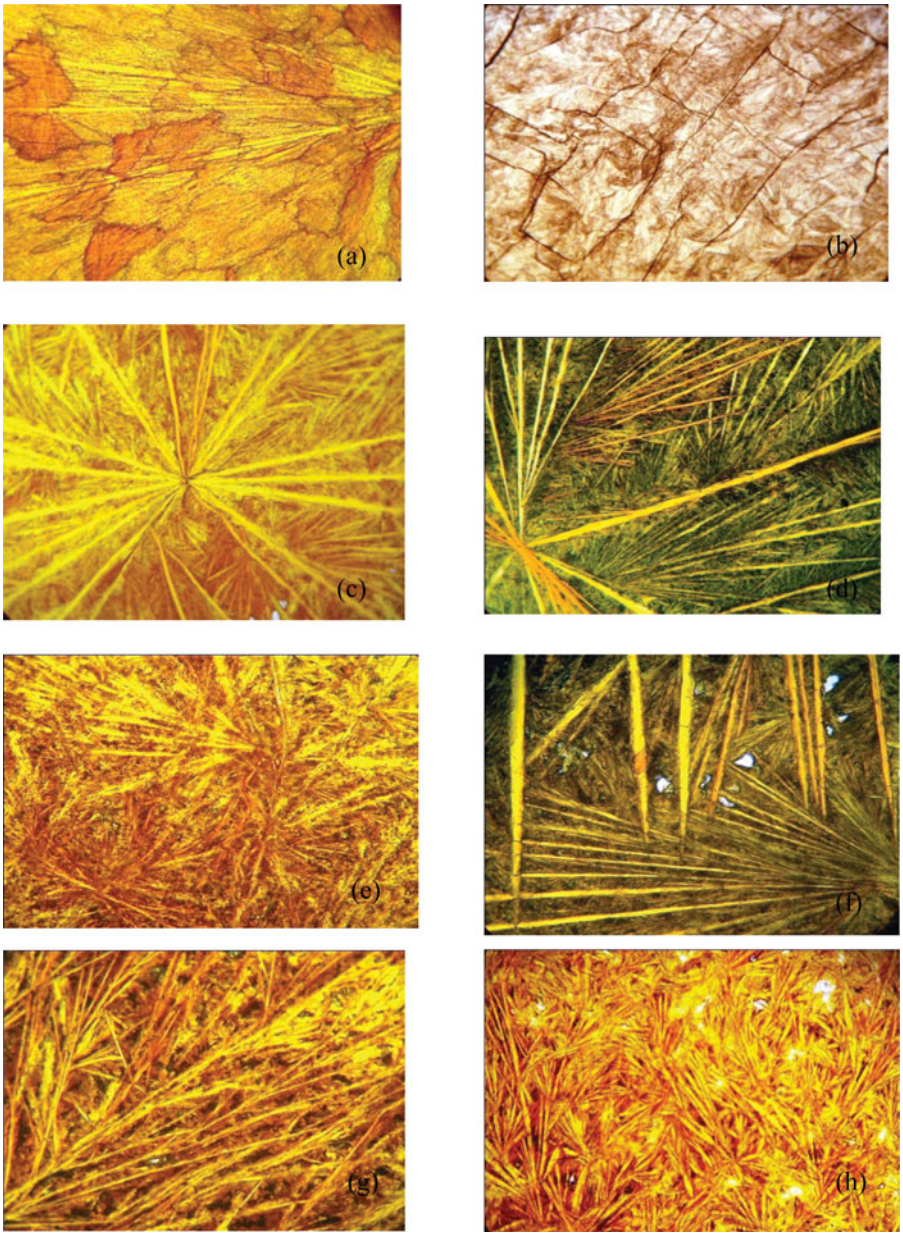

Figure 5. Anisotropic Microstructures: (a) o-nitroaniline (b) β-Naphthol (c) Eutectic, (d) Eutectic with 1% p-Chloranill, (e)Eutectic with 1% Benzoic acid, (f) Eutectic with 1% Naphthalene, (g) Eutectic with 1% Pyrogallol, (h) Eutectic with 1% Phenothiazene.

developed by a eutectic system is governed by the growth characteristics of individual constituent phases. Hunt and Jackson [19] were able to predict the structure of the solid–liquid interface of a material in contact with its liquid with the help of the roughness parameter (α-factor) of the eutectic system by using Eq. (6)

$$\alpha = \xi \frac{\Delta H_{\mathrm{f}}}{\mathrm{RT}} \tag{6}$$

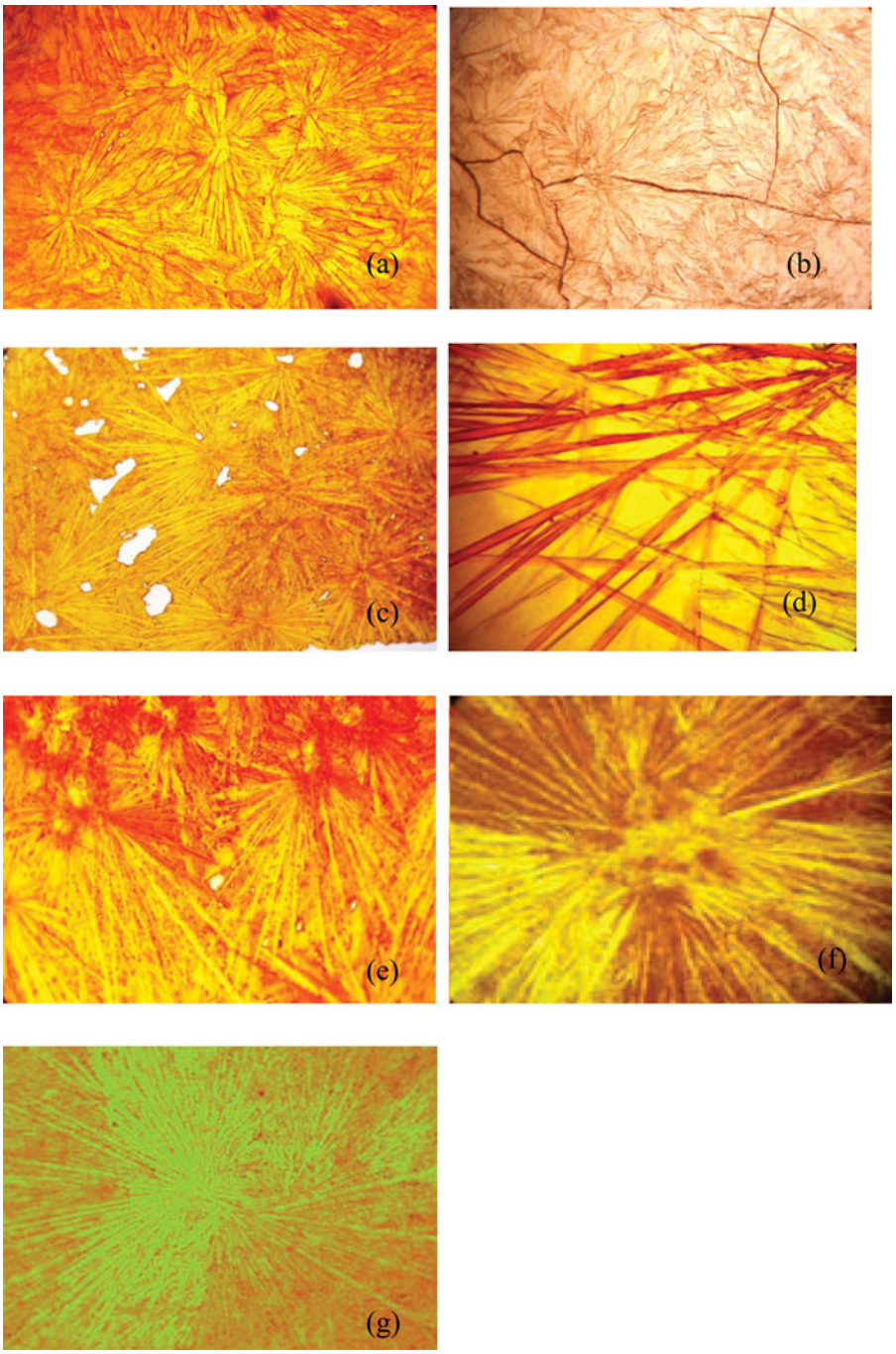

Figure 6. Isotropic Microstructures: (a) o-nitroaniline, (b) β -napthol (c) Eutectic, (d) Eutectic with 1% p-Chloranill, (e)Eutectic with 1% Benzoic acid, (f) Eutectic with 1% Naphthalene, (g) Eutectic with 1% Pyrogallol.

where ξ is a geometrical coefficient often called as crystallographic factor depending upon the geometry of the molecules (ξ lies between 0.5 and 1.0), ΔH_f is heat of fusion and R is gas constant and T is the temperature. The heats of fusion values were determined from DSC curves (Fig. 6). The values of α for the two components and the eutectic mixture were calculated by putting the ξ value equal to 0.5 and 1.0, respectively. Jackson and Hunt [20] reported that

Table 5. Values of modulus of rupture of o-NAN –β-NAPH system.

Components	Modulus of Rupture (MPa)
o-NAN	3.05 ± 0.01
β-NAPH	1.96 ± 0.06
Eutectic	3.86 ± 0.02

for $\alpha > 2$, the solid/liquid interface is atomically smooth and the crystal develops a faceted morphology with an irregular structure. In the present case of 2-NAN, 2-NAPH and eutectic mixture the values of α are greater than 2 (Table 3) and hence show faceted morphology with an irregular structure.

3.6. *Mechanical strength*

Values of modulus of rupture for the systems are given in Table 5. In 2-NAN -2-NAPH system, the results on modulus of rupture show that the flexural strength is experimentally negligible. This may be due to breaking of the cylindrical sample during isotropic growth. The flexural strength of the eutectic material was found to be 3.86 MPa which is higher than the flexural strength of components. This clearly indicates that alignments of components in eutectic composites are more ordered leading to high flexural strength.

3.7. *FT-IR spectral studies*

FT-IR spectral studies revealed the presence of weak interaction between the components in the eutectic mixture. Spectra of 2-NAN showed two sharp peaks at 3474 and 3346 cm^{-1} which was due to the stretching frequency of –N–H of amino group and peaks at 1566 and 1344 cm^{-1} were due to asymmetric stretching frequency and symmetric stretching frequency of $–NO_2$ group, respectively.[21] In the FT-IR spectra of pure 2-NAPH, a small peak appeared at 3501 cm^{-1} due to –OH group.[21] Spectra of 2-NAN -2-NAPH eutectic showed the shifting of the symmetric stretching frequencies of –OH group to lower frequency (3439 cm^{-1} from 3501 cm^{-1}). Furthermore, the two peaks at 1566 and 1344 cm^{-1} shifted to lower frequencies. This indicated the presence of weak hydrogen bonding between H atom of –OH group of 2-NAPH and O atom of $–NO_2$ group of 2-NAN.

4. Conclusion

Phase diagram studies of 2-NAN—2-NAPH showed the formation of eutectic at $X_{2\text{-NAN}} = 0.7222$. Linear velocities of crystallization and thermodynamic parameters indicated that the eutectic mixture is non-ideal in nature and crystallization occurred by side-by-side nucleation of the components. Microstructural studies showed faceted morphology with an irregular structure.

Acknowledgment

The authors are thankful to Prof. S. S. Das and Dr. Preeti Gupta for useful discussions.

References

[1] Meng, G., Lin, X., & Huang, W. (2008). *Mater. Lett.*, *62*, 984–987.
[2] Sharma, B. L. (2003). *Mater. Chem. Phys.*, *78*, 691–701.
[3] Singh, N. B., Agrawal, T., Gupta, P., & Das, S. S. (2009). *J. Chem. Eng. Data.*, *54*, 1529–1536.
[4] Rai, R. N., & Rai, U. S. (2000). *Thermochim. Acta*, *36*, 323–28.
[5] Singh, N. B., Das, S. S. P., & Dwivedi, M. K. (2008). *J. Cryst. Growth*, *311*, 118–122.
[6] Singh, N. B., Giri, D. P., & Singh, N. P. (1999). *J. Chem. Eng. Data*, *44*, 605–607.
[7] Agrawal, T., Gupta, P., Das, S. S., Gupta, A., & Singh, N. B. (2010). *J. Chem. Eng. Data*, *55*, 4206–4210.
[8] Gupta, P., Agrwal, T., Das, S. S., & Singh, N. B. (2012). *J. Chem. Thermodyn.*, *48*, 291–299.
[9] Gupta, P., Agrwal, T., Das, S. S., & Singh, N. B. (2011). *J. Therm. Analys. Calorim.*, *104*, 1167–1176.
[10] Singh, N. B., Das, S. S., Singh, N. P., & Agrawal, T. (2008). *J. Cryst. Growth*, *310*, 2878–2884.
[11] Das, S. S., Singh, N. P., Agrawal, T., Gupta, P., Tiwari, S. N., & Singh, N. B. (2009). *Mol. Cryst. Liq. Cryst.*, *501*, 107–124.
[12] Rastogi, R. P., & Verma, K. T. R. (1956). *J. Chem. Soc.*, *2*, 2097–2101.
[13] Rastogi, R. P., & Bassi, P. S. (1964). *J. Phys. Chem.*, *68*, 2398–2406.
[14] Callister, W. D. Jr. (2005). *Materials Science and Engineering An Introduction*, 6th ed., John Wiley & Sons, Inc.: New York, 412.
[15] Hillig, H. B., & Turnbull, D. (1956). *J. Chem. Phys.*, *24*, 914–920.
[16] Wingard, W. C., Majka, S., & Thall, B. M. (1954). *Can. J. Chem.*, *29*, 320–327.
[17] Singh, N. B., & Dwivedi, K. D. (1982). *J. Sci. Ind. Res.*, *41*, 98–116.
[18] Rastogi, R. P. (1964). *J. Chem. Edu.*, *41*, 443–448.
[19] Jackson, K. A. (1958). *Liquid Metals and Solidifications*, ASM: Cleveland, OH, 174.
[20] Hunt, J. D., & Jackson, K. A. (1966). *Trans. Metall. Soc. AIME*, *236*, 1129–1142.
[21] Silverstein, R. M., Basseler, G. C., & Morrill, T. C. (1991). *Spectrometric Identification of Organic Compound*, John Wiley & Sons Inc.: Canada.